Large Area X-ray Proportional Counter (LAXPC) instrument onboard ASTROSAT

J S Yadav[a1], P C Agrawal[b], H M Antia[a], Jai Verdhan Chauhan[a], Dhiraj Dedhia[a], Tilak Katoch[a], P. Madhwani[a], R K Manchanda[c], Ranjeev Misra[d], Mayukh Pahari[d], B Paul[e], Parag Shah[a]

[a]Tata Institute of Fundamental Research, Homi Bhabha Road, Colaba, Mumbai-400005, India,
[b]CBS, University of Mumbai, Vidyanagari Campus, Kalina, Mumbai-400098, India,
[c]University of Mumbai, Kalina, Mumbai-400098, India,
[d]Inter-university Centre for Astronomy and Astrophysics, Pune-411007, India,
[e]Dept. of Astronomy & Astrophysics, Raman Research Institute, Bengaluru-560080, India

ABSTRACT

ASTROSAT, India's first dedicated astronomy space mission was launched on September 28, 2015. The Large Area X-ray Proportional Counter (LAXPC) is one of the major payloads on ASTROSAT. A cluster of three co-aligned identical LAXPC detectors provide large area of collection. *The large detection volume (15 cm depth) filled with mixture of xenon gas (90%) and methane (10%) at pressure of ~ 2 atmospheres, results in detection efficiency greater than 50%, above 30 keV. The LAXPC instrument is best suited for X-ray timing and spectral studies.* It will provide the largest effective area in 3-80 keV range among all the satellite missions flown so far worldwide and will remain so for the next 5-10 years. The LAXPC detectors have been calibrated using radioactive sources in the laboratory. GEANT4 simulation for LAXPC detectors was carried out to understand detector background and its response. The LAXPC instrument became fully operational on 19th October 2015 for the first time in space. We have performed detector calibration in orbit. The LAXPC instrument is functioning well and has achieved all detector parameters proposed initially. In this paper, we will describe LAXPC detector calibration in lab as well as in orbit along with first results.

Keywords: X-rays and radio, X-ray space instrument, ASTROSAT, LAXPC, X-ray fast variability, Micro quasars, Pulsars, detector calibration, X-ray timing, X-ray spectroscopy

[1] jsyadav@tifr.res.in; phone 91 22 2278 2253; fax 91 22 2280 4610; www.tifr.res.in

Space Telescopes and Instrumentation 2016: Ultraviolet to Gamma Ray, edited by
Jan-Willem A. den Herder, Tadayuki Takahashi, Marshall Bautz, Proc. of SPIE Vol. 9905, 99051D
· © 2016 SPIE · CCC code: 0277-786X/16/$18 · doi: 10.1117/12.2231857

Downloaded From: http://spiedigitallibrary.org/ on 08/19/2016 Terms of Use: http://spiedigitallibrary.org/ss/termsofuse.aspx

1. INTRODUCTION

ASTROSAT is India's first dedicated astronomy space mission which was launched on September 28, 2015. The Large Area X-ray Proportional Counter (LAXPC) is one of the major payloads on ASTROSAT. For X-ray timing and low-resolution spectral studies over a broad energy band (3-80 keV), ASTROSAT will use a cluster of three co-aligned identical LAXPC each with a multi-wire-multi-layer configuration and a Field of View better than 1^o X 1^o [1]. The LAXPC is a large and complex X-ray instrument (8 flight packages with about 120 electronic cards) which has been designed and developed at TIFR. *To achieve the scientific objectives, several interesting and innovative approaches are employed which include:*

1. *LAXPC instrument uses large detection volume of 15 cm depth filled with xenon gas at two atmospheres pressure to achieve high detection efficiency in 3-80 keV energy range.*

2. Three independent and modular electronics systems for three LAXPC Detectors to ensure high reliability and adequate safety measures against single-point failures.

3. All three detectors use a common and accurate time reference.

4. To achieve low detector background, various logics are used to reduce backgound based on (a) Level Discrimination (b)Mutual coincidence & (c) Anti coincidence.

5. Extensive calibration with radioacitve sources in laboratory in scanning mode using remotely controlled calibration unit.

6. GEANT4 simulation of detector response, detector background and the collimator field of view.

The LAXPC instrument consists of three identical units, each with its own independent front-end electronics, HV supply, and signal processing electronics. The Time mark generating electronic unit is common for all the three LAXPCs. The data from all the LAXPCs are independently acquired preserving the identity of each unit. These data are merged in a single telemetry data stream from which data for each LAXPC is recovered.. *The LAXPC instrument is a low resolution, broadband spectroscopy detector with large collection area.* Each LAXPC detector consists of the following major parts:

(i) Detector and the detector housing

(ii) Back plate of the detector housing

(iii) Collimator (Window support collimator (WSC) and Field of view (FOV) collimator)

(iv) On-board gas purification unit with solenoid valves and plumbing

Downloaded From: http://spiedigitallibrary.org/ on 08/19/2016 Terms of Use: http://spiedigitallibrary.org/ss/termsofuse.aspx

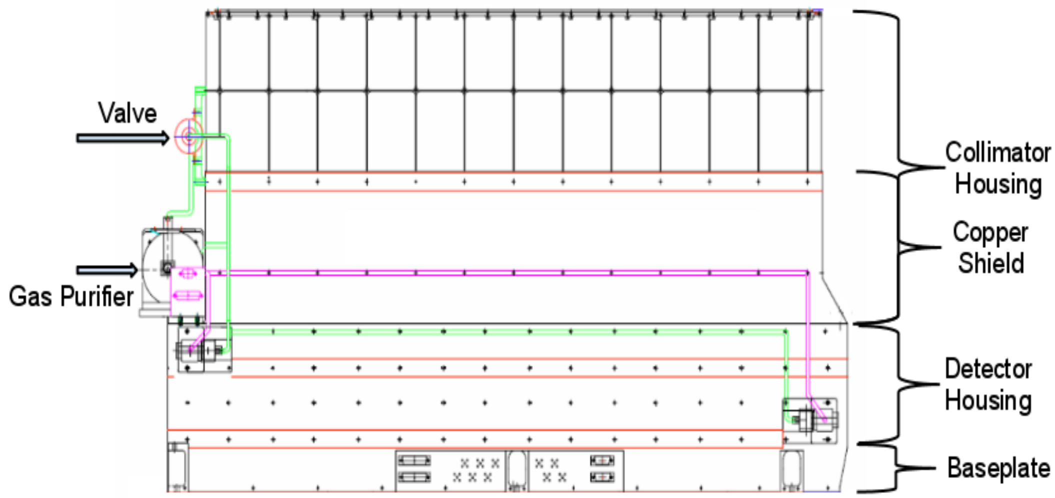

Figure 1: Schematic diagram of LAXPC detector with major detector parts

The Front End Electronics is housed in the milled out pockets on the back plate of LAXPC detector. Each of the detectors is biased with their corresponding high voltage units mounted on the back plate. The Front End package also has its corresponding low voltage DC-DC converter mounted on the back plate. Each of the LAXPC detector has an onboard gas purification system. This system will be periodically operated to purify the gas content of the detector. The Drive electronics for all three bellow pump motors is housed in common package of LAXPC Bellow Drive

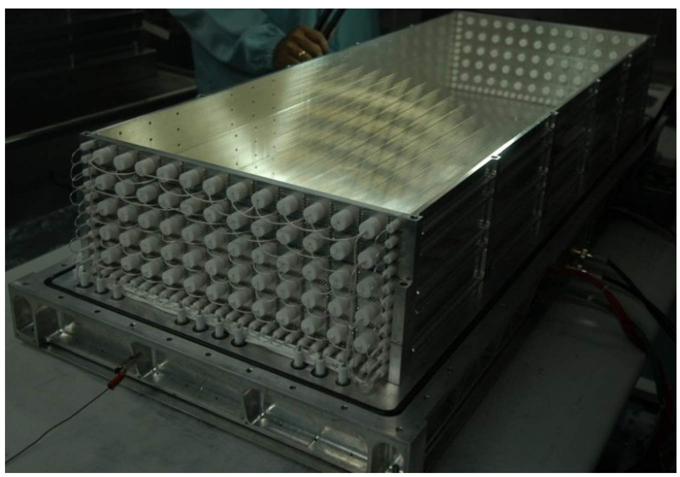

Figure 2; Main and anti anode layers in LAXPC detector

Downloaded From: http://spiedigitallibrary.org/ on 08/19/2016 Terms of Use: http://spiedigitallibrary.org/ss/termsofuse.aspx

Table 1: LAXPC instrument specification

No. of LAXPC Detector	Three Identical units
A Detector Size	120cm x 50cm x 70cm
X-ray detection volume	100cm x 36cm x 15cm
No. of Anode layers	5 anode layers each of 12 anode cell surrounded on 3 sides with Veto cells
Instrument Veto layers	46 anode cells each with cross-section of 1.5 cm x 1.5 cm arranged on three sides of X-ray detection cells
Collimator field of view	55′X 55′ for all the LAXPCs
Collimator Height	45 cm for WSC+FOV collimator
Counting Gas	Xenon (90%) + Methane (10%)
Gas Pressure	Two atmosphere (1520 torr)
Energy range	3-80 keV
Total Effective Area of 3 LAXPC Detectors	About 6000 cm^2 in 5-20 keV
Total Weight of LAXPC	414 Kg (Detector + Electronics)

Each LAXPC detector consists of 60 anode cells of 3 cm x 3 cm cross-section and length of 100 cm, arranged in 5 layers providing a 15 cm deep X-ray detection volume. Each Anode Layer thus has 12 anodes with a total width of 36 cm [3]. A Veto Layer made up of 46 anode cells each with cross-section of 1.5 cm X 1.5 cm surrounds the main X-ray detection volume on three sides to reject events due to charged particles and interaction of high energy photons in the detector. The alternate anode cells of Layer 1 and 2 are linked together which results total four outputs. The anode cells in each of the Layer 3, 4 and 5 are linked together to provide one output from each layer. Thus there are 7 anode outputs that are operated in mutual anticoincidence to reduce the non-cosmic X-ray background. The Veto layer is divided in three parts (left side, right side and bottom) providing 3 Veto Layer outputs. To suppress background from charged particles all events which register in multiple anodes or those which trigger the veto anodes are rejected, except for the situation where one of the energies is in the K X-rays for Xenon. For X-rays with energy above the K-edge of Xe, a K-electron may be ejected and the ion can radiate a K X-ray photon in energy range 29-34 keV. These X-ray may escape from the detector or be absorbed in a different anode. In order to include such events the anti-coincidence logic is modified to detect this energy range. If two main anodes register an event and at least, one of them is in the energy range of 25-35 keV, then the energy of the two anodes are added and the event is accepted. The lower threshold for this (KLLD) and the upper

Downloaded From: http://spiedigitallibrary.org/ on 08/19/2016 Terms of Use: http://spiedigitallibrary.org/ss/termsofuse.aspx

threshold (KULD) can be set through tele-command. A blocking shield (1 mm tin + 0.2 mm Cu) is used on four sides and bottom to reduce background further.

There are seven anode outputs from the X-ray detecting cells and three veto outputs from each detector that are fed to ten charge sensitive preamplifiers (CSPAs). High voltage to the anodes is supplied from a command controlled HV unit whose HV output can be varied by command. The outputs from the CSPAs are sent to the peak detectors and events satisfying the selection logic as true X-ray events are further processed by signal processing electronics. This is a part of processing electronics. The signals generated by the instrument after detection of X-rays are processed and stored in any of the following modes.

- Normal (or Default) Modes of Operation :

  In Normal operation there are two modes running simultaneously and data are acquired from each LAXPC.

  (a) Broad Band Counting Data: Records the rate of occurrence of events in various energy bands with selectable time bin (16 msec to 2048 msec). Default value is 128 msec.

  (b) Event Mode Data: In this mode arrival time of each event is time tagged to an accuracy of 10 microseconds. Simultaneously, the energy and identity of each event is also recorded. This mode generates 5 bytes data for each accepted and analyzed event. In this mode the dead time of the detector is around 50 microseconds.

- Fast Counter Mode: In this mode the event rate is measured only from the top layer of each LAXPC detector in 4 energy channels covering 3-20 keV band with a fixed time bin of 160 microsecond. In this mode dead time is about 10 microsecond. Each of 4 counters are 8 bit deep and cover 3-6, 6-8 , 8-12 and 12-20 keV energy bands. This mode is to be used for studying rapid variability at very high flux.

Figure 3: All the three LAXPC Space flight detectors in Assembly, integration and testing lab (AIT) lab after successfully completing all flight tests and final calibration (20th October, 2014). The purification pump is seen as black box in each detector.

Downloaded From: http://spiedigitallibrary.org/ on 08/19/2016 Terms of Use: http://spiedigitallibrary.org/ss/termsofuse.aspx

2. LAXPC DETECTOR CALIBRATION ON GROUND

Each of the LAXPC detectors has an onboard gas purification system. This system will be operated as and when required to purify the gas filled in the detector by command. It is expected that energy resolution of LAXPC detector will degrade as impurity increases. The impurity rate is expected to be more in the lab than that in orbit. We have tested purification system in the laboratory and figure 4 shows the improvement in detector resolution after purification of LAXPC30 in laboratory.

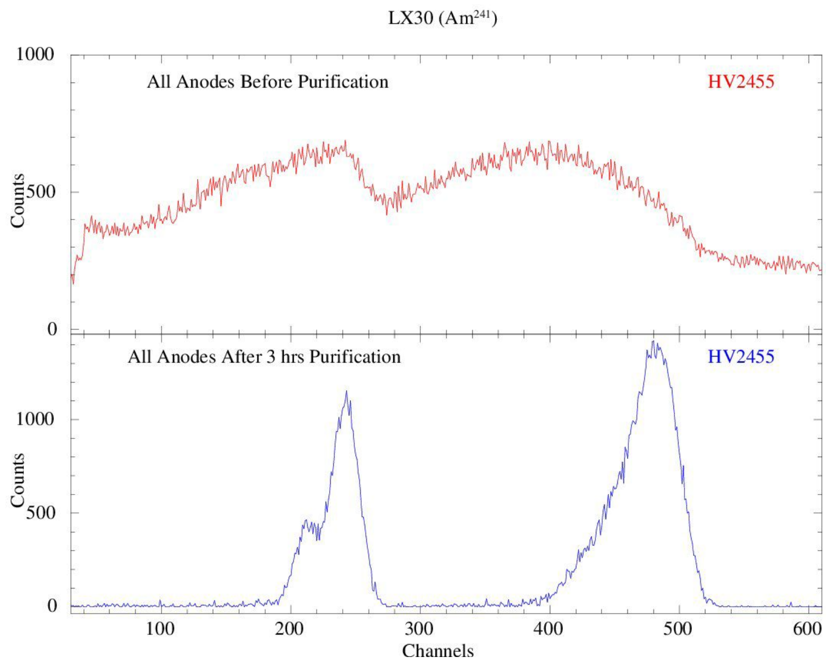

Figure 4: LAXPC30 detector energy resolution before (top) and after (bottom) purification.

In order to perform the calibration inside a thermovac chamber, an X-Y motion calibration unit for movement of radioactive sources above the field of view collimator was designed. This can hold up to three sources and expose one or more of them at a time. The movement is controlled remotely and can be programmed. *We have used scan mode which is close to the mode in orbit as it averages the performance over whole detector area. We used* three radioactive sources, Fe^{55} (6 keV), Cd^{109} (22 keV, 25 keV) and Am^{241} (60 keV) for estimating the detector response and energy resolution.

Downloaded From: http://spiedigitallibrary.org/ on 08/19/2016 Terms of Use: http://spiedigitallibrary.org/ss/termsofuse.aspx

The calibration was repeated at temperatures of 10 C, 20 C and 30 C to study the temperature dependence of energy resolution and peak position. Figure 5 shows the measured energy resolution as a function of energy for LAXPC10 for three temperature. *The black line shows single anode results and we have achieved LAXPC detector performance as proposed initially.*

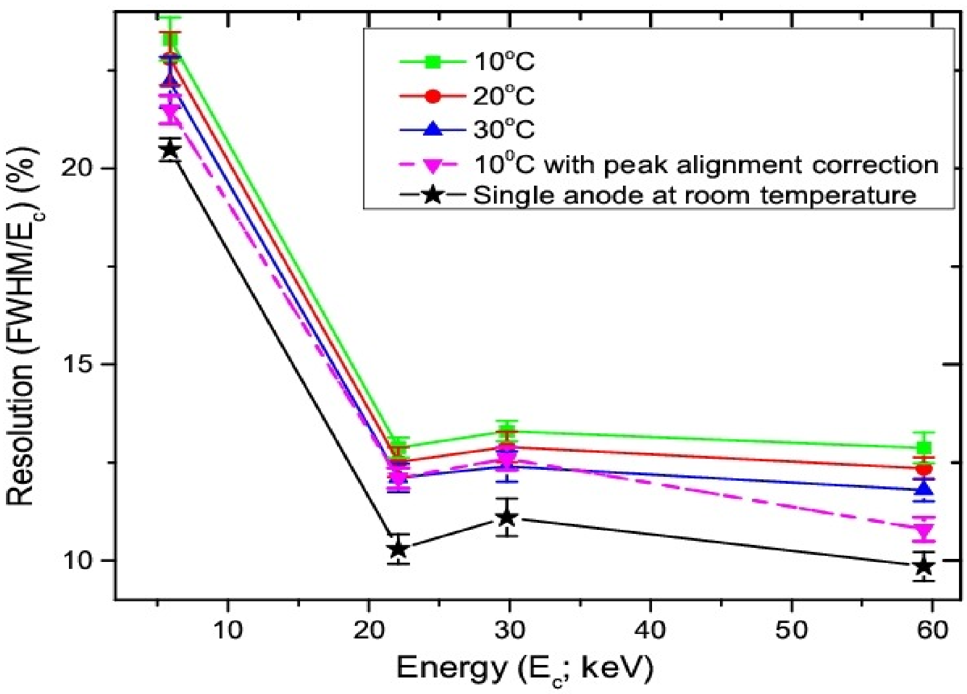

Figure 5: The energy resolution for 6, 22, 30 and 60 kev at three temperature measured in scan mode (averaged over whole detector). The energy resolution for single anode at 20 C is shown in black.

2.1. GEANT4 simulation

The GEANT4 simulations of the LAXPC detectors were carried out to understand the detector response. The details of the simulation are described in a previous report (Antia et al. 2013) and also in calibration document for LAXPC10. For each radioactive source the known energy distribution was used in the simulation. Each simulation had 10^6 photons which were incident perpendicular to the top-face of the detector. The detector response was first calculated for each of the three radioactive sources and results were compared with observed spectra. The simulated spectrum of Am^{241} source in LAXPC30 is shown in figure 7 (red) and compared with measured spectrum (black). The simulated spectra has been normalized to give the same total counts. The energy resolution for each peak and the energy to channel mapping were kept as free parameters in

Downloaded From: http://spiedigitallibrary.org/ on 08/19/2016 Terms of Use: http://spiedigitallibrary.org/ss/termsofuse.aspx

simulation to match the observed spectra. The channel number was modelled as a quadratic function of energy. These spectra matches well and hence validate our simulated detector response.

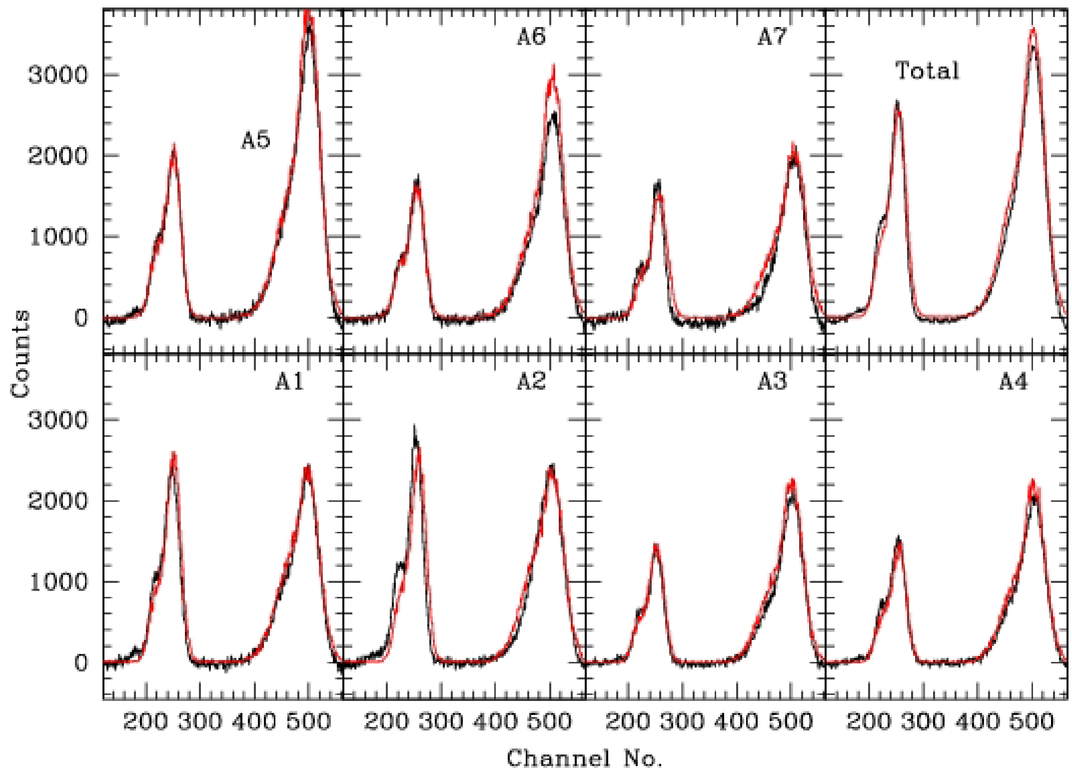

Figure 6: Simulated (red) and measured (black) spectra for Am^{241} source in LAXPC30 detector at 10^{o} C.

The energy resolution and channel to energy mapping of all detectors was estimated by fitting the calibration results for the three radioactive sources and the result is shown in Figure 7.

Detection efficiency is determined by the thickness of entrance window at the low energy end and by the probability of photoelectric interaction in the detector gas volume at the higher energy end. GEANT4 simulations of detector have been used to estimate the effective area and field of view. The simulations were validated by comparing the simulations with observations using radioactive sources. Once the energy resolution and channel to energy mapping are known, it is possible to use GEANT4 simulation with different incident energies to determine the detector response.

Downloaded From: http://spiedigitallibrary.org/ on 08/19/2016 Terms of Use: http://spiedigitallibrary.org/ss/termsofuse.aspx

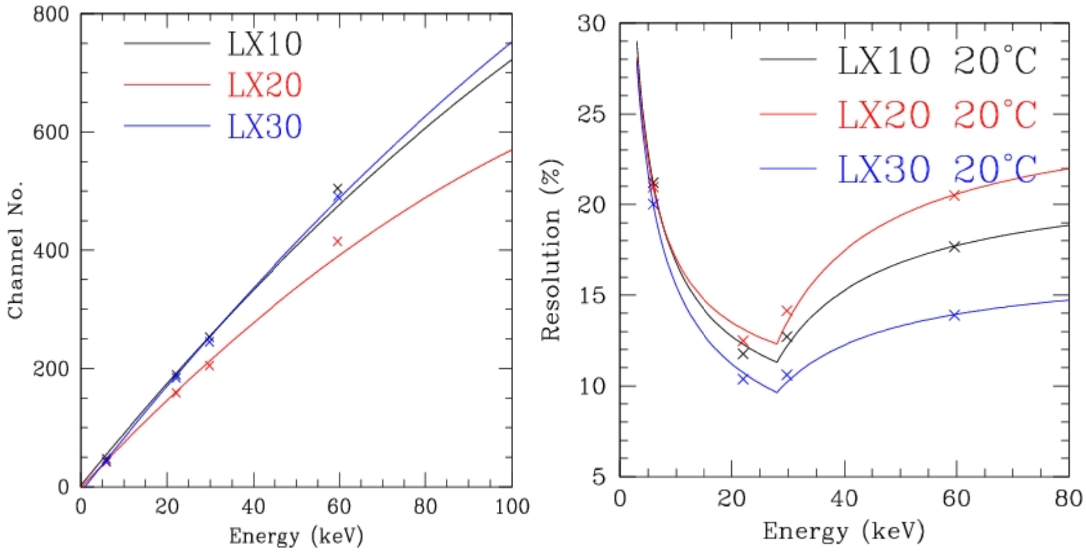

Figure 7: The resolution and peak position for the three LAXPC detectors at 20 C obtained\by fitting the spectra for three radioactive sources to simulations.

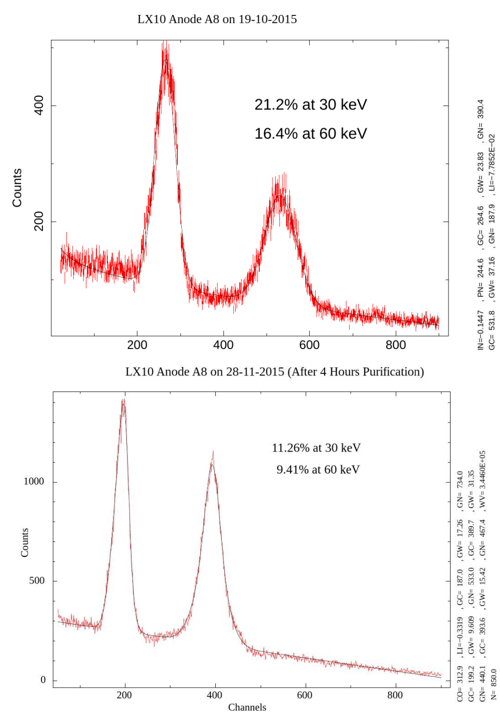

Figure 8: LAXPC 10 detector energy resolution before and after purification of detector gas (upper and lower panels respectively) obtained from on-board Am source located in a veto anode.

Downloaded From: http://spiedigitallibrary.org/ on 08/19/2016 Terms of Use: http://spiedigitallibrary.org/ss/termsofuse.aspx

3. LAXPC DETECTOR CALIBRATION IN ORBIT

The LAXPC instrument subsystems; the system based time generator (STBG), processing electronics and low voltage detector electronics were switched on during 29 September- 1st October, 2015. The LAXPC payload was fully functional on 19th October, 2015 when high voltage (HV) of all three LAXPC detectors was switched on. Onboard LAXPC detector purification was operated during 20-22 October, 2015 and 23-24 November, 2015. Energy resolution of LAXPC10 was degraded to around 21 % at 30 keV and after gas purification in orbit, energy resolution improved to around 11% (figure 8).

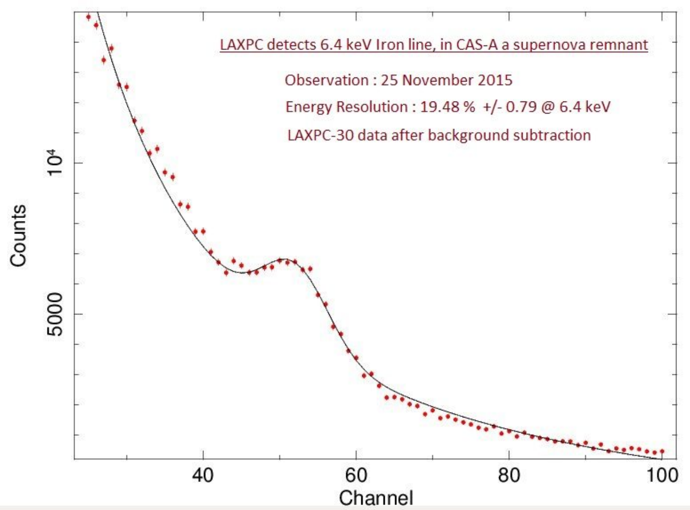

Figure 9: CAS –A (Supernova remnant) observation of LAXPC30. We have achieved ~20% energy Resolution at 6.4 keV.

LAXPC observation of CAS A is shown in Figure 9 which suggest around 20% energy resolution at 6.4 keV Iron line. LAXPC observation of GX 301-2 also clearly resolved Iron line. A number of standard sources were observed to understand and fine tune the detector characteristics. Since ASTROSAT is in an equatorial orbit at an altitude of about 650 km, the charged particle flux is generally low, except during passage through the South Atlantic Anomaly (SAA) where the high voltage in the detector is switched off. To model the detector background, blank sky regions were observed over a period of 1 day on several occasions. The background counts vary by 10%-20% in orbit, with counts increasing close to SAA region. To model the background we assume that the count rate is a function of latitude and longitude. The resulting model matches the observed counts to within 3%. The average background counts are about 250 s^{-1} for LAXPC10 and 200 s^{-1} for other detectors. The higher count rate in LAXPC10 is because one of the veto anodes in this detector is not functioning. The observed background spectrum is close to what was obtained by GEANT4 simulations using diffuse cosmic X-ray background.

Downloaded From: http://spiedigitallibrary.org/ on 08/19/2016 Terms of Use: http://spiedigitallibrary.org/ss/termsofuse.aspx

A scan across the Crab X-ray source was used to estimate the field of view of the detector which is determined by the collimator geometry. The FWHM of the detector is found to about 55' which is close to what was estimated by GEANT4 simulations using collimator geometry. The observed spectrum of the Crab X-ray source was used to calibrate the response matrix. The energy to channel mapping was fine tuned to match the Crab spectrum and the results for LAXPC10 are shown in Figure 10.

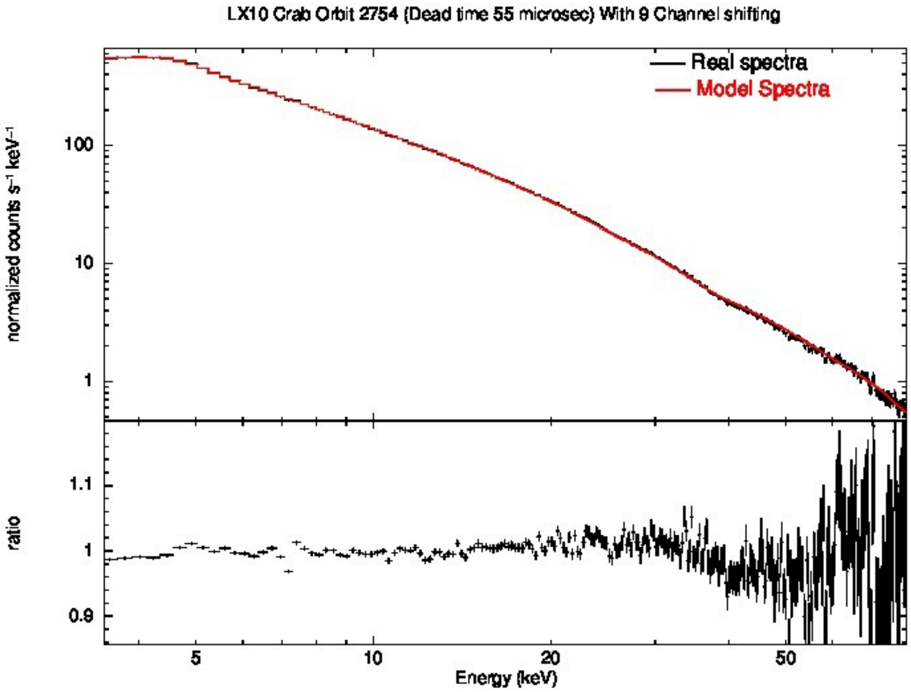

Figure 10: Fit to observed spectrum of Crab X-ray source for LAXPC10.

The black line in upper panel shows the observed spectrum after subtracting the background and the red line shows the fitted spectrum using the response matrix for the detector assuming a power law. The lower panel shows the ratio. The fitted spectrum matches the observed spectrum to within 2% over most of the energy range of 3-80 keV. It gives power law index 2.08 with normalization 7.9 and reduced chi-square ~ 1.5 over 3-80 keV energy range. The response matrix for all three detectors is obtained by similar process. The final normalization to calculate the effective area needs to be fixed by cross-calibration with other instruments. Preliminary results of these calibration appear to suggest a total effective area of about 6000 cm^2 when the three detectors are combined. Detailed study of cross calibration data is in progress.

To test the timing characteristics of the detector, event mode data which gives the arrival time and energy of each photon to a time-resolution of 10 microsec is used to calculate the power density spectrum up to the Nyquist frequency of 50 kHz. The resulting spectrum does not show any instrumental effect other than peaks beyond 10 kHz due to dead-time of the detector which was estimated to be about 50 microsec on ground. Comparing the observed spectrum with expected spectrum from a non-paralyzable detector yields a dead-time of 42.3 microsec. A detailed timing

Downloaded From: http://spiedigitallibrary.org/ on 08/19/2016 Terms of Use: http://spiedigitallibrary.org/ss/termsofuse.aspx

study of black-hole source GRS 1915+105 confirms high quality of data, which is only limited by the Poisson statistics and the dead-time effects.

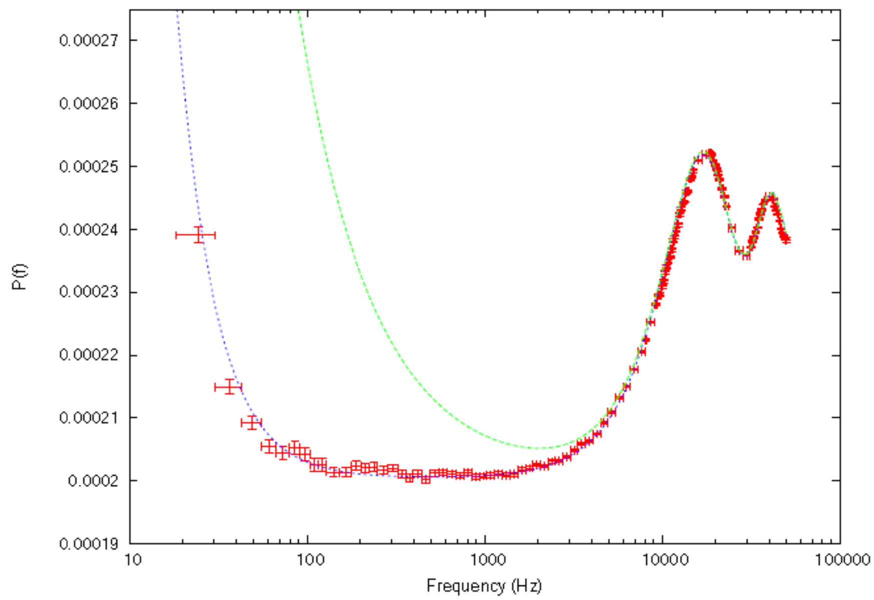

Figure 11: The high frequency rebinned power density spectra of GRS 1915+105 in SPL state. The green line shows the expected peak power of a QPO with quality factor Q=4 and rms of 5%.

4. FIRST RESULTS:

The LAXPC instrument has advantage of better detection efficiency than PCA/RXTE above 30 keV and fine timing capabilities. We observed large number of X-ray sources during PV phase which ended on 31st March, 2016. These X-ray sources include pulsars, micro quasars, LMXBs, HMXBs, clusters, supernova remnants, AGNs etc. We have observed 4U 0115+63 a pulsar with cyclotron line in outburst. Figure 12 shows the light curve observed in three LAXPC detectors with PDS. Figure 13 shows PDS with QPOs in different energy bands observed in GRS 1915+105 in SPL X-ray state [5]. These results shows that LAXPC instrument can explore higher energy bands with sufficient power.

We have observed thermonuclear bursts in 4U 1636-536 and in 4U1728-34 which are shown in Figure 14. These data are being further analyzed. We have observed radio loud theta X-ray class in GRS 1915+105 where transient radio jets are produced. Figure 15 shows light curve in top panel, and hardness ratio HR1 and HR2 in middle and bottom panels. We have simultaneously observed radio jets with GMRT during 6-7 March, 2016 [6]. The power density spectrum (PDS) of Crab with its pulse profile in different energy bands is shown in Figure 16. We have observed high frequency QPOs in 4U 1728-34 and GX 1826-24. We are also detecting gamma ray bursts in LAXPC instrument most of them entering from sides as increased background.

Downloaded From: http://spiedigitallibrary.org/ on 08/19/2016 Terms of Use: http://spiedigitallibrary.org/ss/termsofuse.aspx

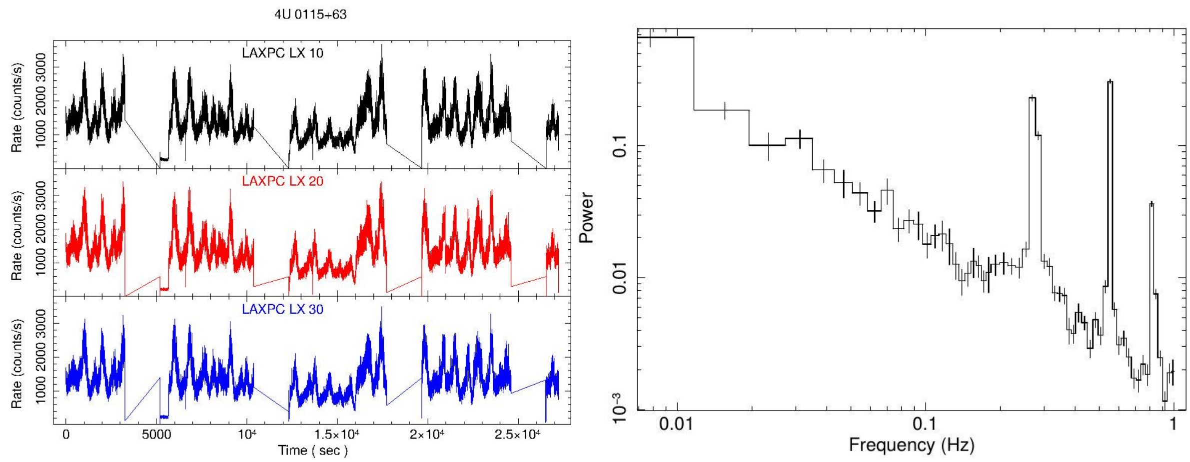

Figure 12: The light curve of 4U 0115-63 in outburst observed in three LAXPC detectors. Left panel show PDS its spectrum.

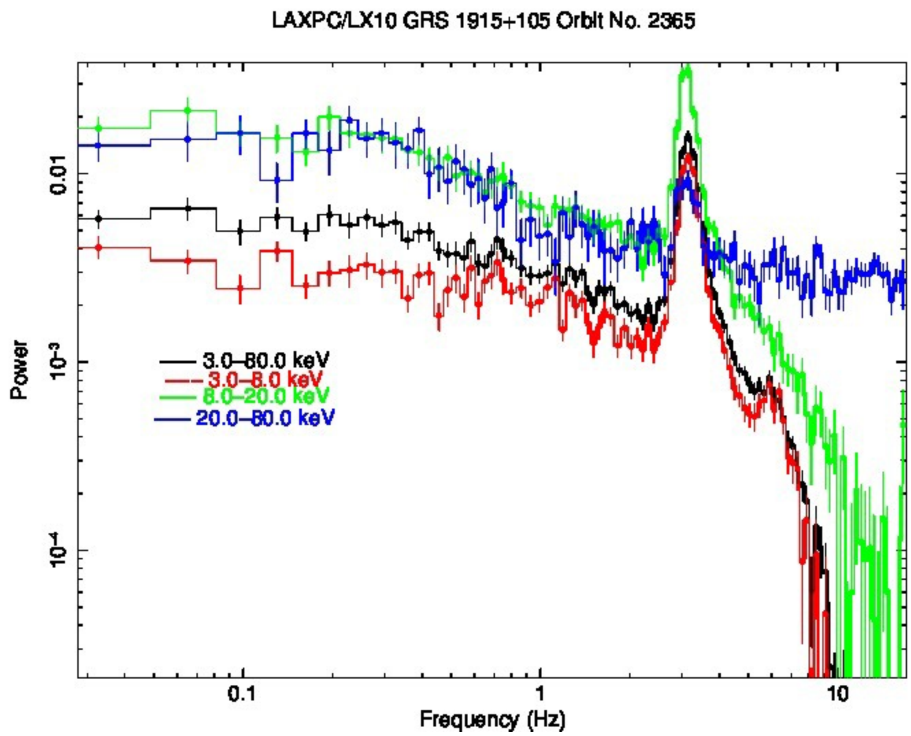

Figure 13: PDS observed in LAXPC10 with QPOs in different energy bands observed in GRS 1915+105 in SPL X-ray state.

Downloaded From: http://spiedigitallibrary.org/ on 08/19/2016 Terms of Use: http://spiedigitallibrary.org/ss/termsofuse.aspx

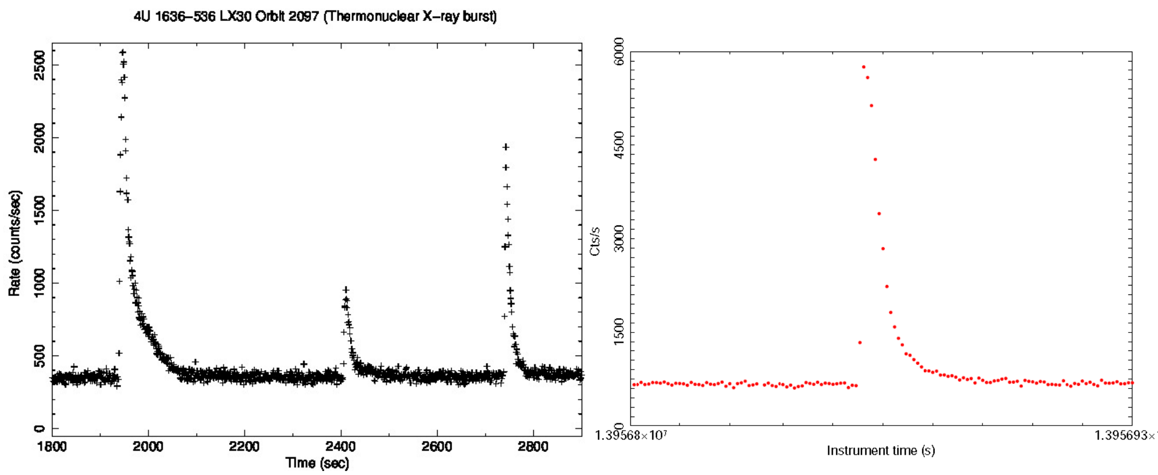

Figure 14: Thermonuclear burst observed in 4U 1636-536 and in 4U1728-34

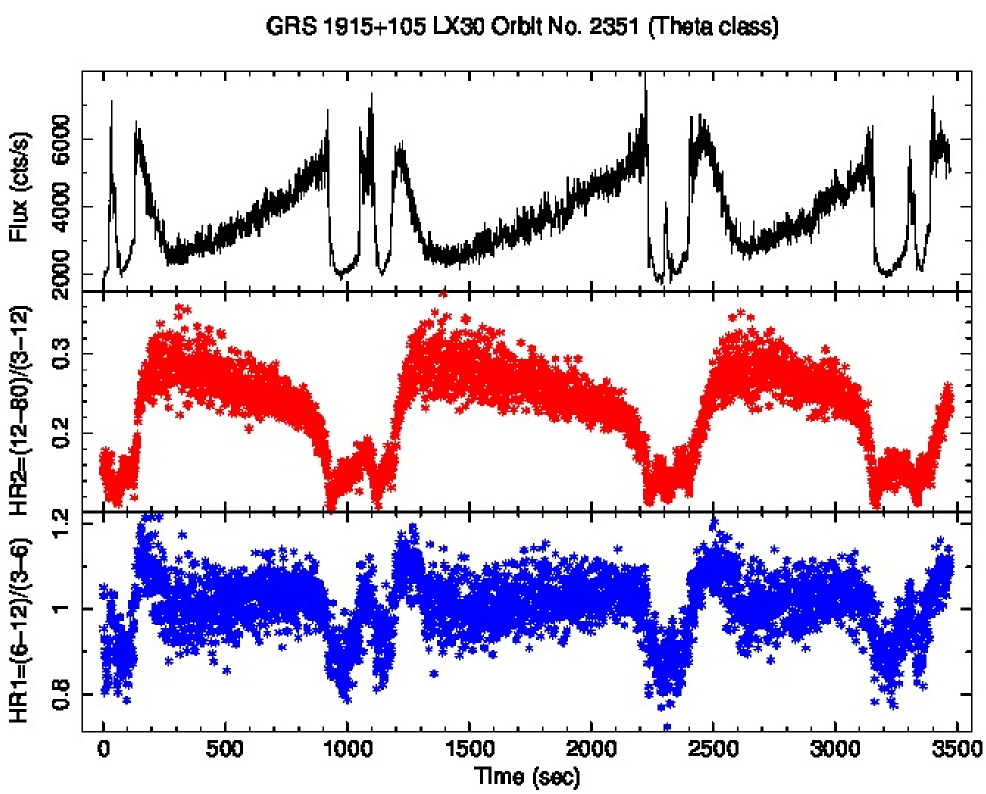

Figure 15: LAXPC observation of GRS 1915+105 in theta class. Transient radio jets are observed with GMRT simultaneously.

Downloaded From: http://spiedigitallibrary.org/ on 08/19/2016 Terms of Use: http://spiedigitallibrary.org/ss/termsofuse.aspx

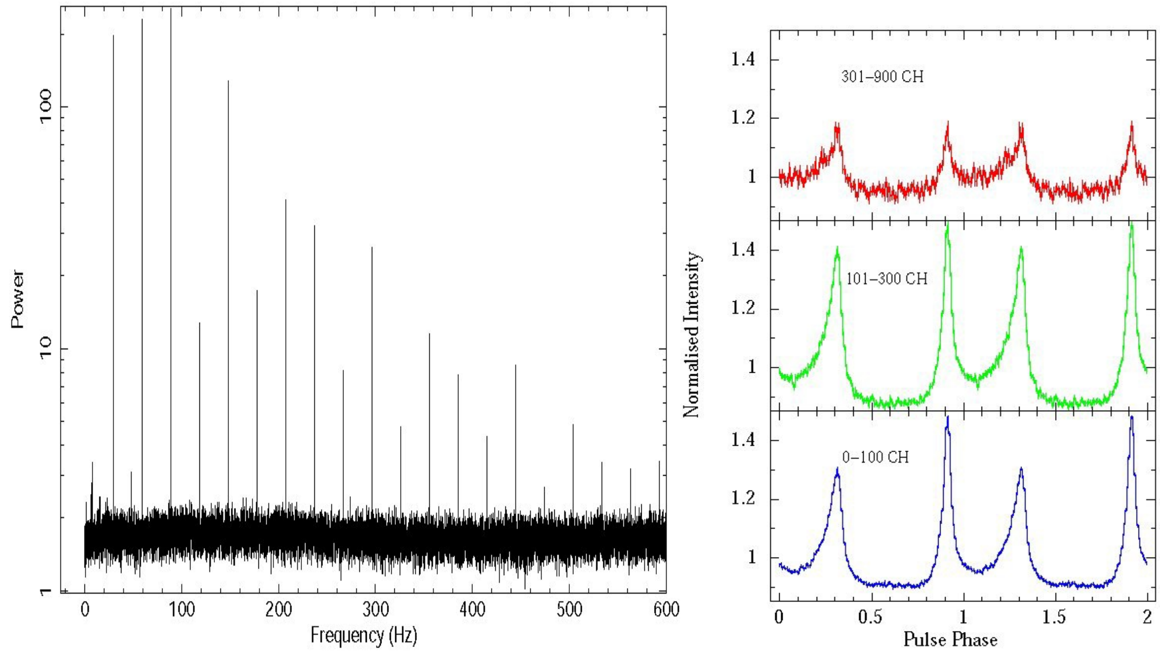

Figure 16: The PDS spectrum of Crab is shown in left panel and its pulse profile in different energy bands is shown in right panel.

Acknowledgement: We acknowledge the strong support from ISAC/ (ISRO) in various aspect of instrument building and testing. *We specially appreciate all support from Mr. V Koteswara Rao, Mr. K Suryanarayana Sarma , Mr K Navalgund and other members of Project team. We thank* IISU *for* providing us with bellow pump and the space qualified pump driver. We thank SAC Ahmedabad group for software development. We also acknowledge support of TIFR central workshop during the design and testing of the payload.

References:

[1] P C Agrawal, AdSR 38 (2006) 2989.

[2] H M Antia, V R Chitinus, T VKatoch, I Mazumdar, M Pahari, S Wadawale, J S Yadav (2013) GEANT4 simulation of LAXPC background (technical report).

[3] LAXPC/ASTROSAT CDR report, LAXPC team, January, 2014 TIFR/AST/LAXPC/CDR-01.

[4] K Johoda et al , 2006 ApJS 163, 401.

[5] J S Yadav, 2006 ApJ 648, 385.

[6] Mayukh Pahari et al 2013, ApJ 778,136.

Downloaded From: http://spiedigitallibrary.org/ on 08/19/2016 Terms of Use: http://spiedigitallibrary.org/ss/termsofuse.aspx